Environmental Pollution 363 (2024) 125246

Contents lists available at ScienceDirect

Environmental Pollution

journal homepage: www.elsevier.com/locate/envpol

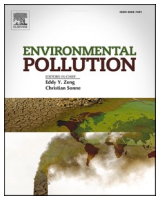

Effects of nanoplastics on the growth, transcription, and metabolism of rice *(Oryza sativa* L.) and synergistic effects in the presence of iron plaque and humic acid

Xiaoxue Ouyang [a,b,c], Jie Ma [b,c,*], Bingcong Feng [b,c], Yong Liu [b,c], Ping Yin [a], Xiaoyu Zhang [b,c], Pan Li [d], Qiusheng Chen [a], Yujie Zhao [b,c], Liping Weng [c,e], Yongtao Li [f]

[a] Institute of Agricultural Product Quality, Safety and Nutrition, Tianjin Academy of Agricultural Sciences, Tianjin, 300381, China
[b] Key Laboratory for Environmental Factors Control of Agro-Product Quality Safety, Ministry of Agriculture and Rural Affairs, Tianjin, 300191, China
[c] Agro-Environmental Protection Institute, Ministry of Agriculture and Rural Affairs, Tianjin 300191, China
[d] School of Earth System Science, Tianjin University, Tianjin, 300072, China
[e] Department of Soil Quality, Wageningen University, Wageningen, the Netherlands
[f] College of Natural Resources and Environment, South China Agricultural University, Guangzhou, 510642, China

ARTICLE INFO

Keywords:
Nanoplastics
Oryza sativa L.
Root iron plaque
Humic acid
Multiomics

ABSTRACT

Nanoplastics (NPs) can adversely affect living organisms. However, the uptake of NPs by plants and the physiological and molecular mechanisms underlying NP-mediated plant growth remain unclear, particularly in the presence of iron minerals and humic acid (HA). In this study, we investigated NP accumulation in rice (*Oryza sativa* L.) and the physiological effects of exposure to polystyrene NPs (0, 20, and 100 mg L^{-1}) in the presence of iron plaque (IP) and HA. NPs were absorbed on the root surface and entered cells, and confocal laser scanning microscopy confirmed NP uptake by the roots. NP treatments decreased root superoxide dismutase (SOD) activity (28.9–44.0%) and protein contents (31.2–38.6%). IP and HA (5 and 20 mg L^{-1}) decreased the root protein content (20.44–58.3% and 44.2–45.2%, respectively) and increased the root lignin content (22.3–27.5% and 19.2–29.6%, respectively) under NP stress. IP inhibited the NP-induced decreasing trend of SOD activity (19.2–29.5%), while HA promoted this trend (48.7–50.3%). Transcriptomic and metabolomic analysis (Control, 100NPs, and IP-100NPs-20HA) showed that NPs inhibited arginine biosynthesis, and alanine, aspartate, and glutamate metabolism and activated phenylpropanoid biosynthesis related to lignin. The coexistence of IP and HA had positive effects on the amino acid metabolism and phenylpropanoid biosynthesis induced by NPs. Regulation of genes and metabolites involved in nitrogen metabolism and secondary metabolism significantly altered the levels of protein and lignin in rice roots. These findings provide a scientific basis for understanding the environmental risk of NPs under real environmental conditions.

1. Introduction

Nanoplastics (NPs) are small plastic debris (less than 1 μm) and represent a new environmental contaminant that has been the subject of considerable research in recent years (Gigault et al., 2018; Liao et al., 2022). They exist widely in the environment and have been observed to enter plant roots and translocate to the aerial parts of the plant (Lian et al., 2021; Hartmann et al., 2022; Wang et al., 2022b; Zhang et al., 2022). For example, polystyrene (PS) NPs (100–700 nm) can be taken up by the root systems of cucumber and transported through the stems to the leaves, flowers, and fruits (Li et al., 2021). Exposure to PS NPs (50 nm) leads to PS NPs internalization within the vacuoles, cytoplasm, and nucleus of roots cells in *Allium cepa* (Giorgetti et al., 2020). Moreover, micro-sized plastics can enter plant roots via endocytosis or discontinuous regions in the Casparian strip. A scanning electron microscopy (SEM) characterization revealed the presence of micro-sized (2 μm) PS microbeads in the leaf veins of lettuce and wheat (Li et al., 2020). NP properties, such as the components, sizes, surface charge, and properties, can influence the uptake and translocation of NPs in plants (Wang et al., 2022a). For example, as the particle size decreases, NPs show a

* Corresponding author. Key Laboratory for Environmental Factors Control of Agro-Product Quality Safety, Ministry of Agriculture and Rural Affairs, Tianjin, 300191, China.
E-mail address: majie@caas.cn (J. Ma).

https://doi.org/10.1016/j.envpol.2024.125246
Received 12 August 2024; Received in revised form 29 October 2024; Accepted 4 November 2024
Available online 4 November 2024

greater tendency to enter plant structures (Liu et al., 2022). Certain plants like *Arabidopsis thaliana* preferentially absorb negatively charged NPs (PS-COOH) over positively charged NPs (PS-NH_2) (Sun et al., 2020). However, the electrostatic attraction of PS-NH_2 on the cell wall of negatively charged maize leaves is stronger than that of PS-COOH (Sun et al., 2021). Many studies have reported that NPs not only affect the growth, development, and reproduction of plants but also disturb their normal metabolism (Shen et al., 2019; Gao et al., 2023). For instance, PS-NPs reduce root elongation and induce morphotoxicity and cytogenotoxicity in *Allium cepa* (Maity et al., 2020). Moreover, NPs directly threaten human health through ingestion, inhalation, and skin contact, causing various risks that range from cytotoxicity, inflammation, oxidative stress, and diseases including cancer (Atugoda et al., 2022; Lee et al., 2023b). Although increasing attention is being focused on the toxicity of NPs for terrestrial plants and human beings, their environmental impacts and underlying mechanisms remain unclear.

Rice (*Oryza sativa* L.) is the world's second largest food crop after wheat worldwide. It is planted over the widest area and provides food for more than half of the global population. Studies have confirmed that NPs can affect rice growth, enter rice roots, and translocate to the grain, eventually harming human health through the food chain (Zhou et al., 2021; Jiang et al., 2022; Lima et al., 2023). Nano-sized polystyrene can be absorbed by rice roots, translocated to the aerial parts via the apoplast pathway, and accumulate in the vascular systems of plant tissues (Liu et al., 2022). NPs at 10 mg L^{-1} are taken up by the rice roots, where they significantly enhance antioxidant enzyme activity, decrease the root length, and increase the lateral root numbers, activate carbon metabolism, and inhibit jasmonic acid and lignin biosynthesis (Zhou et al., 2021).

Rice grows in flooded environments, and iron oxide plaque (IP) naturally forms on the root surface through a reaction between oxygen, oxidants, and soluble reductive Fe^{2+}, which is a layer of amorphous or crystalline iron (oxyhydr) oxides on the root surface (Sebastian and Prasad, 2016; Fu et al., 2018). In addition to acting as a buffer and reservoir for nutrient uptake, IP can increase the adsorption capacity of roots for heavy metals (Cu, Cd, Cr, Zn, and As) and nanoparticles while sequestering heavy metals and nanoparticles on the root surface. This layer acts as a barrier layer for plants in the uptake of heavy metals and nanoparticles (Williams et al., 2014; Li et al., 2017b; Yang et al., 2020). Iron minerals, such as goethite, hematite, and magnetic iron nanoparticles, can affect the bioavailability and migration behavior of NPs in the environment through adsorption and coprecipitation (Li et al., 2019; Zhang et al., 2020; Adeleye et al., 2023). Nonetheless, the interactions between IP and NPs and how they may influence the fate of NPs have not been clarified.

Humic acid (HA) is as a typical organic matter that generally exists in natural water, where its concentration ranges from 20 μg L^{-1} in groundwater to 30 mg L^{-1} in surface water (Black et al., 1996; Hemati et al., 2012). Moreover, it is an important component in the regulation, immobilization, and transport of contaminants and colloids (Wang et al., 2012; Ma et al., 2018a; Xiong et al., 2018). Numerous negatively charged functional groups on the surface of HA (such as carboxyl (-COOH) and hydroxyl (-OH)) can increase both the negative surface charges on NPs and electrical repulsion, generate steric hindrance to restrain aggregation, and enhance the mobility of NPs (Dong et al., 2021; Tan et al., 2021). Our previous results showed that agricultural organic inputs and iron minerals can also effectively control the transport of 50 nm NPs (Ma et al., 2022). In addition, because iron oxide and HA have opposite charges, the addition of HA may significantly affect the metal ion adsorption capacity of iron oxides (Kang and Xing, 2008; Li et al., 2017a). Therefore, it is important to investigate the impact of HA on the transport and behavior of NPs in the presence of iron minerals.

In addition to affecting the movement of NPs as typical compounds in rice fields, IP and HA may regulate the entry of NPs from roots to plants (Nie et al., 2023). However, the comprehensive effects of IP formation and HA on NP uptake and translocation in rice exposed to NPs have rarely been studied. Furthermore, the phenotypic and molecular mechanisms through which IP formation and HA affect NP uptake by rice are poorly understood. Therefore, for a more complete understanding of the influencing processes and mechanisms of IP and HA, this study analyzed the uptake, translocation, and toxicological effects of NPs in environment-rice systems under NPs exposure. To achieve this, we evaluated the biochemical phenotypic effects on rice (including root/shoot length, plant weight, enzyme activities, organic acid, protein laccase, and lignin) within a hydroponic culture of NPs, IP, and NP-IP/HA and NP-IP-HA mixtures and assessed the deposition of NPs on the surface of rice roots, and studied the distribution of NPs in the roots using various microscopic techniques. Additionally, transcriptomic and metabolomic analyses were also performed to evaluate the underlying mechanism of NP toxicity in rice at the molecular level, both in the presence and absence of IP and HA. Our findings contribute to providing a more realistic assessment of the environmental risks of NPs and offer new insights into conducting joint environmental risk assessments of NPs, natural iron minerals, and HA.

2. Materials and methods

2.1. Experimental materials

Carboxyl-modified fluorescence (green) polystyrene NPs used in the study were purchased from Huge Biotechnology, Shanghai, China (particle size: ~20 nm; variable coefficient <5%; spherical shape) as a 10% w/v suspension dissolved in ultrapure water. The NP morphology was characterized using transmission electron microscopy (TEM, JEM-2100F, JEOL) (Fig. S1a). The zeta potential of NPs measured by a laser diffraction particle size analyzer (Zetasizer Nano ZS, Malvern) was −18.8 ± 0.57 mV at 25 °C and pH 7.0. To minimize any possible interference caused by residual surfactants in the NP suspension, dialysis was carefully performed. Ferrihydrite (FH) was synthesized (Jia et al., 2007; Qian et al., 2020), and HA was purified from commercial humus following the classical alkali/acid procedure (Valdrighi et al., 1996). The X-ray diffraction pattern of the solid confirmed the synthesized FH (Fig. S1b). HA properties were characterized in our previous study (Ma et al., 2018b). Ferrihydrite nanoparticle (FH_N) and HA suspensions were prepared by ultrasonic dispersion after adding 0.4 g FH and 2.0 g HA to 400 mL Milli-Q water, respectively. The complete details are shown in Supporting information (SI) 1.

Rice seeds (*Oryza sativa* L., Yudao 16) were obtained from Henan Agricultural University (Henan, China), and Hoagland's nutrient solution used for the rice culture was purchased from Shanghai Yuanye Bio-Technology Co., Ltd. Seedling details are provided in SI 2. The seedlings were grown in the solution until the three-leaf stage, and no obvious IP formation was noted. All seedlings were divided into two parts, with half transferred into flat-bottom glass tubes containing 100 mg L^{-1} FH_N nutrient solution to induce IP formation and the other half treated as previously described. In this process, 100 mg L^{-1} FH_N did not exhibit significant toxicity to rice. After IP was formed (Fig. S2), the seedlings were rinsed three times with ultrapure water to remove the residual iron (Fe) on the surface of roots. The results of a scanning electron microscopy equipped with energy-dispersive X-ray spectroscopy (SEM-EDS, OxfordX-MAX, Zeiss) confirmed the formation of IP and revealed the presence of Fe on the root surface of rice (Fig. S3). Finally, all seedlings were transferred to flat-bottom glass tubes containing 20 mL ultrapure water and starved for 5 d.

2.2. Nanoplastic exposure experiment

Ten treatment groups were established, and the experimental design is described in Table 1. Working NP suspensions (20 and 100 mg L^{-1}) were prepared by adding NP aliquots to 40 mL of 1/2 Hoagland's nutrient solution, which was then homogenized by sonication for 30

Table 1
Design of nanoplastic exposure experiment.

Treatments	Iron plaque (IP)	NP concentrations ($mg{\cdot}L^{-1}$)	HA concentrations ($mg{\cdot}L^{-1}$)	Label
1	–	0	0	CK
2	–	20	0	20NPs
3	–	100	0	100NPs
4	–	100	5	100NPs-5HA
5	–	100	20	100NPs-20HA
6	with	0	0	IP
7	with	20	0	IP-20NPs
8	with	100	0	IP-100NPs
9	with	100	5	IP-100NPs-5HA
10	with	100	20	IP-100NPs-20HA

min. The seedlings were subsequently transferred to a nutrient solution and cultured in an artificial climate box (day/night photoperiod, temperature, and relative humidity were 14 h, 30 °C, 80% and 10 h, 24 °C, 80%, respectively). Given that plant exposure experiments are usually performed for 7–14 d (Zuverza-Mena et al., 2017), the NP exposure experiment was conducted for 15 d in this study. Each treatment was set up in five replicates, and each tube contained one seedling. The concentrations of the NP suspensions were determined based on data from previous studies (Chae and An, 2020; Maity et al., 2020; Zhou et al., 2021). The concentration of the FH_N and HA solution was determined based on our preliminary experiments and data in the literature (Black et al., 1996; Li et al., 2016; Liu et al., 2021a). The NP concentration of the solution was measured five times (1, 3, 6, 10, and 15 d) based on a 0.5 mL sample using an ultraviolet and visible spectrophotometer (UV-2700, Shimadzu, Kyoto, Japan) at 300 nm. The calibration curve for the NPs and NP−HA concentrations vs. absorbances is provided in Fig. S4. After harvesting, the accumulation of NPs on the root surfaces was evaluated by visualizing the unwashed root surfaces using SEM-EDS, with either spots of interest examined or scanning mode applied. To confirm the uptake of NPs by rice roots, the cellular NP distribution in the root tips of the CK, 100NPs, and IP-100NPs treated groups were evaluated using the confocal laser scanning microscopy (CLSM, FV1200, Olympus) by excitation with an argon laser at 488 nm (green). The complete descriptions are available in SI 3.

2.3. Biochemical, metabolomic, and transcriptomic analyses

Fresh plants were thoroughly washed with deionized water and ultrapure water to remove the NPs adhered on the root surface, then divided into roots and shoots. The root/shoot height and fresh weight of each tissue were measured. The superoxide dismutase (SOD), catalase (CAT), and peroxidase (POD) activities and protein, laccase, and lignin contents of the rice plants were determined using kits purchased from Comin Biotechnology Co., Ltd, China. A complete description is available in SI 4. High-performance liquid chromatography (HPLC, UltiMate 3000, Thermo Fisher Scientific) was used to measure organic acid content (including oxalate acid, tartaric acid, citric acid, malic acid, propanedioic acid, and succinic acid). A complete description is available in SI 4.

Tissue samples (roots and shoots) of CK, 100NPs, 100NPs-20HA, IP, IP-100NPs, and IP-100NPs-20HA were selected for metabolomic analysis, and the ultra-high-performance liquid chromatography coupled with time-of-flight mass spectrometry (UHPLC-TOF-MS, Triple TOF 5600+, AB SCIEX) was employed to screen for metabolites. A complete description is available in SI 5. Moreover, tissue samples (roots and shoots) from CK, 100NPs, and IP-100NPs-20HA groups were obtained for transcriptome analysis. Total RNA was extracted from three biological replicates using the TRIzol® Reagent (Invitrogen, Carlsbad), RNA sequencing was conducted using an Illumina NovaSeq 6000 platform at Shanghai Majorbio Biopharm Biotechnology Co., Ltd. (Shanghai, China), and the raw sequences and differentially expressed genes (DEGs) were obtained using the online platform of Majorbio Cloud Platform. The complete description of the methods is available in SI 5.

2.4. Statistical analyses

Statistical analyses and the figures were performed using the SPSS 17.0 and R software version 4.0.3. Significant differences between variables were determined using a One-way analysis of variance (ANOVA) followed by the Tukey's HSD test. $P < 0.05$ was considered as a significant difference. The NPs characterization, root length, shoot height, fresh weight, enzyme and metabolomic content data were presented as the mean value ± standard deviation (SD) of at least three replicates in each treatment.

3. Results and discussion

3.1. Root surface deposition and uptake of NPs

To understand the root surface deposition and uptake of NPs, changes in the NP concentration within the solution and the distribution of NPs on the root surface and in the roots were analyzed in the presence of IP and HA.

The NP concentration in the solution of each group decreased during culture (Fig. 1a). On day 15, almost no NPs was detected in the solution of the high-concentration NP groups (100NPs and IP-100NPs). Although relatively slow, 81% of settlement was achieved in the low concentration NP groups (20NPs). A slight dose-dependent relationship was observed between the settlement rate and the exposure concentration of NPs. The average settlement rate of NPs in the presence of IP (98.9%) was higher than that in the absence of IP (94.1%) (Fig. 1a), indicating that IP slightly promoted NP deposition. Generally, IP comprises amorphous or crystalline iron oxides or hydroxides, and their surface hydroxyl groups can undergo proton migration and exhibit ampholytoid properties, ultimately leading to NP adsorption (Tan et al., 2021). A previous study showed that positively charged Fe/aluminum (hydr) oxide minerals can interact with negatively charged polystyrene NPs to form heteroaggregates and decrease the stability of polystyrene NP colloidal suspension (Zhang et al., 2020; Nie et al., 2023). The IP on the rice root surface interacted with the negatively charged NPs through electrostatic interactions and ligand exchange, thereby increasing the adsorption and accumulation of NPs on the rice root surface. The SEM results showed that NPs were loaded onto the rice root surface, both in the presence or absence of IP (Fig. S5). However, more NPs were adsorbed onto the root surface when the NP solution was applied in the presence of IP (Fig. 1a). IP sequestered most of the NPs in the IP groups, thereby preventing direct contact between the roots and NPs. Furthermore, NPs attached to the IP surface exerted electrostatic repulsion to suspended NPs in the solution, further inhibiting the heteroaggregation of NPs (Quevedo et al., 2013). IP may serve as a substantial energy barrier to block the uptake of NPs by roots. However, although the epithelial cells were covered with IP, NPs still penetrated the epithelial root cells. CLSM was employed to study the accumulation of NPs in rice roots (Fig. 1c). The green fluorescence signal of NPs was observed for both the treatment and control groups at 488 nm, and the auto-fluorescence was observed in the rice roots. The fluorescence signals were greater in the intercellular and intracellular spaces of the roots in the treatment groups compared to those in the CK. NPs had clearly entered and accumulated in the rice roots. A previous study using CLSM also observed NPs distributed in rice root tips (Zhou et al., 2021). A number of studies have indicated that very tiny NPs (e.g., ≤60 nm) enter root cells through liquid-phase endocytosis and cell wall pores (Chae

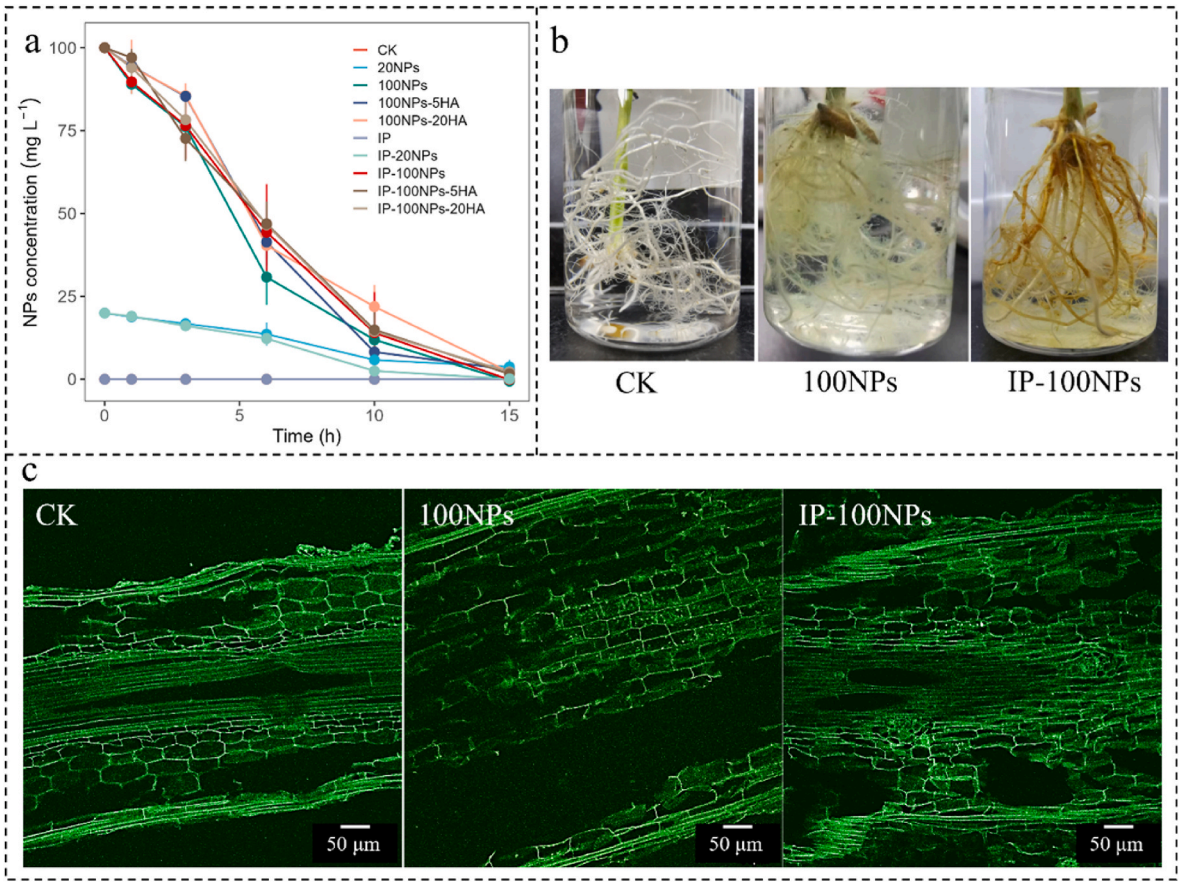

Fig. 1. (a) Time-dependent concentration of NPs in solution under different treatments; (b) images of NPs deposited on the root surface of rice (*Oryza sativa* L.) under CK, 100NPs and IP-100NPs groups; (c) Confocal laser scanning microscopy (CLSM) images of rice roots under CK, 100NPs and IP-100NPs groups.

and An, 2020; Lian et al., 2020), while relatively larger particles (few hundred nanometres to several micrometres) enter root tips mainly through the rhizome or epidermis via an intercell-wall route (Jiang et al., 2019; Zhang et al., 2019; Sun et al., 2020). Surface charges may also affect the uptake and distribution of NPs by plants. Due to electrostatic attraction from the negatively charged cell wall, positively charged NPs are likely to be deposited on root cell walls, while negatively charged NPs are not (Wu and Li, 2022). Moreover, negatively charged NPs occur more frequently in the apoplast and xylem (Sun et al., 2020). Aging NPs are more hydrophilic and less electronegative (Prust et al., 2020), thus enabling them to enter cells in a manner similar to negatively charged NPs. In addition, because of aggregation promoted by the growth medium and root exudates, positively charged NPs can aggregate into larger particles than negatively charged NPs (Sun et al., 2020). In the present study, although negatively charged NPs showed significantly decreased mobility due to aggregation, they could still enter the root cells. Generally, HA can restrain the aggregation of NPs and heteroaggregation between NPs and iron/aluminum (hydr)oxide minerals (Li et al., 2018; Dong et al., 2021; Nie et al., 2023). However, in this study, the presence or absence of HA had little effect on NP aggregation (Fig. 1a); thus, its inhibitory effect was negligible.

NPs can be absorbed onto the root surface and enter the cell, and IP enhanced the deposition of NPs on the root surface. NPs entering the roots are translocated to the aerial parts of the plant, directly and indirectly influencing plant growth and performance, such as biomass, shoot height, and root length (Lima et al., 2023).

3.2. Impact of NPs on rice growth and physiological characteristics

The length and biomass of rice seedlings under different treatments are presented in Fig. S6. After 15 d of cultivation, the root length, shoot length, and fresh weight of rice had increased compared to those on day 1 (Fig. S6). On day 15, the root length of each treatment group had increased compared to that of the CK group, but the changes were not obvious (Fig. S6a). Similarly, no significant changes were found in the shoot length and fresh weight of rice seedlings under any of the treatments compared with the CK group. A previous review indicated that in over 40% of cases, MPs/NPs did not cause significant variations in root and shoot height and biomass compared to the control (Lima et al., 2023). In this study, the environmental factors of IP and HA did not significantly enhance the toxic effects of NP exposure on rice seedling growth. This could be attributed to the effects of NPs on plant growth, which depend on contamination levels, soil, and plant characteristics (Wang et al., 2022a). The nutrient solution provided good nutritional support for seedling growth, and the NPs had no obvious adverse effects on rice morphological phenotypes.

Oxidative damage is one of the primary ecotoxicological mechanisms induced by NPs (Hartmann et al., 2022; Wang et al., 2022b), and the levels of SOD, CAT, and POD in rice tissues were determined after 15 d (Fig. 2, Fig. S7). NPs significantly reduced the SOD contents of the roots by 28.9–44.0% compared to the CK group (Fig. 2a), indicating that oxidative stress caused by NPs may have exceeded the scavenging abilities of SOD and induced the excessive accumulation of ROS. A similar study found that the SOD activities of rice were decreased after exposure to a 0.2 g L^{-1} of polystyrene and polytetrafluoroethylene (Dong et al., 2020). A dose-dependent relationship between NPs and SOD contents were observed, and the SOD content decreased with an increasing NP concentration (Fig. 2a); this was attributed to the NPs inducing dose- and size-dependent oxidative stress (Liu et al., 2021b; Wang et al., 2022a). The SOD activities of rice roots (*Oryza sativa*) were

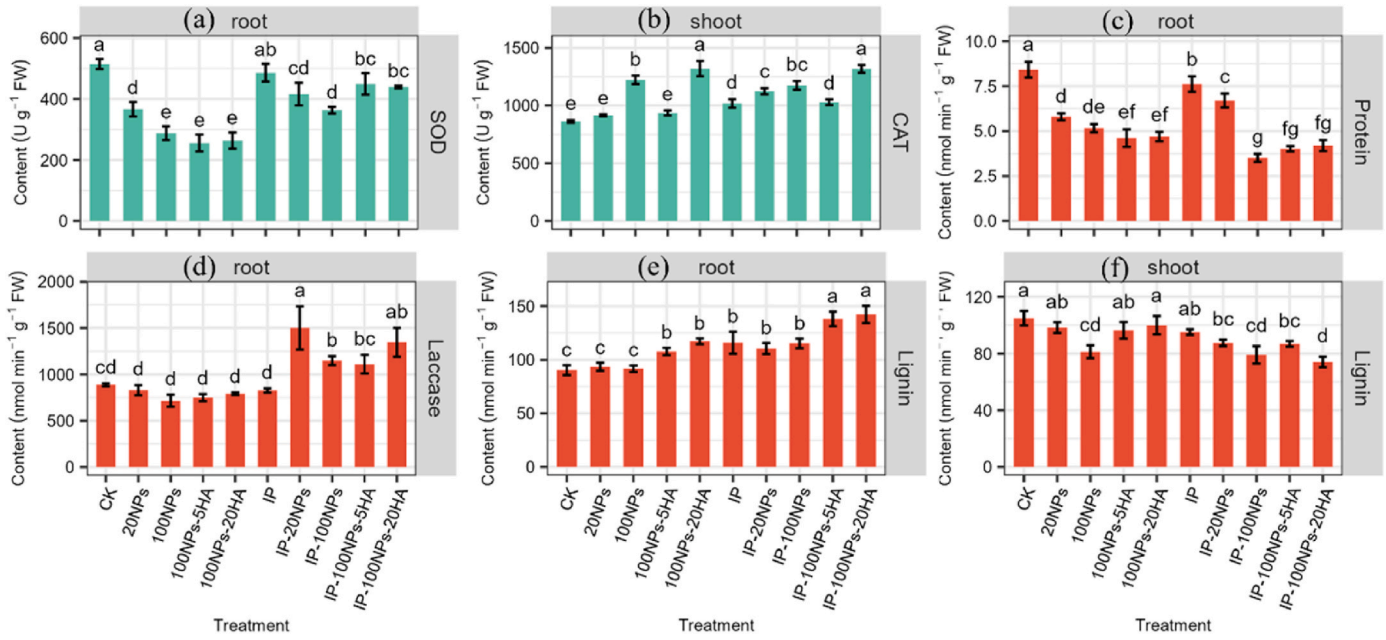

Fig. 2. Contents of (a) superoxide dismutase (SOD) in rice (*Oryza sativa* L.) roots and (b) catalase (CAT) in rice shoots; (c)–(e) contents of protein, laccase, and lignin in rice roots; (f) contents of lignin in rice shoots; The values were given as mean ± SD (standard deviation). Different letters (a, b, c) indicated values significantly different under the different treatments ($p < 0.05$, ANOVA with Tukey's HSD, $n = 5$).

significantly stimulated by 50 and 100 mg L^{-1} NPs compared to 10 mg L^{-1} (Zhou et al., 2021). With an increase in the NP concentration, the CAT contents of the roots and shoots increased, but no differences were observed in the roots (Fig. S7a), whereas the CAT contents of shoots increased by 5.0–41.0% compared to the CK group (Fig. 2b). There were no significant differences between the POD contents of roots and shoots across all treatments (Figs. S7c–d). This suggested that SOD and CAT, but not POD, were the main antioxidant enzymes in the roots and shoots under NP treatments. In addition, under NP stress, IP and HA decreased the SOD contents of roots by 19.2–29.5% and by 48.7–50.3%, respectively, compared with the CK group (Fig. 2a). Thus, IP shielding of NPs may have alleviated oxidative stress in the roots, whereas HA had the opposite effect.

The effects of NPs on the organic acid, protein, laccase, and lignin contents were analyzed (Fig. 2 and Figs. S8–9). NPs had no significant effect on the root acid content in the presence or absence of IP and HA (Fig. S9). In the roots, NPs had an adverse effect on the protein content, which decreased by 32.2–38.6% compared to the CK group (Fig. 2c). Although the lignin content increased slightly under NP exposure, it was not significant (Fig. 2e). Increases in the protein content of microalga *Scenedesmus quadricauda* (Li et al., 2023) and the lignin content in lettuce roots (Lei and Engeseth, 2022) under NP exposure have been reported in previous studies. In this study, IP significantly affected the root protein, laccase, and lignin contents. The protein contents of the roots in the IP groups were lower than those in the absence of IP groups (average 10.1%) under NP stress (Fig. 2c). In contrast, the laccase (average 43.3%) and lignin (average 18.9%) contents were higher than those in the absence of IP (Fig. 2d and e). Under NP stress, the presence of IP reduced the protein content and increased the laccase and lignin contents of the roots. Meanwhile, HA significantly decreased the protein content by 44.2–45.2% and increased the lignin content of roots by 19.2–29.6%, compared to the CK group (Fig. 2c and e). An increase in proteins (particularly soluble proteins) and their accumulation can improve the water-holding capacity of cells and protect the important substances and cell biofilms (Junaid and Wang, 2021). Laccase is the key enzyme of lignin precursors involved in polymerization (Kärkönen and Koutaniemi, 2010), which polymerize monolignols into p-hydroxyphenyl (H), guaiacyl (G), and syringyl (S) units, thereby affecting the lignin content. Lignin is the main constituent of plant cell walls, and changes in its content is related to plant cell wall thickness (Day et al., 2009). NPs can stimulate thickening of the algal cell wall, thereby blocking the entry of NPs (Mao et al., 2018). Excessive ferrous ions may be toxic to plants during IP formation on the root surface, thereby decreasing the protective effect of IP (Ward et al., 2008). This can be attributed to the decreased protein content and increased lignin content in the roots of the IP and IP-containing groups in our study. Furthermore, the hydroponic conditions in the laboratory differed from the actual conditions. In this study, only FH was loaded on the rice root surface, whereas the root surface under natural conditions contains a variety of minerals; therefore, the effect of IP in this experiment may be more significant than the actual condition. Even though a greater amount of IP reduced the absorption of NPs by rice roots, the IP on the roots may still serve as the primary storage of NPs. The addition of HA reduced the aggregation between NPs and IP, enhanced the activity of NPs, and facilitated the entry of NPs into the roots. This entry caused oxidative stress in the plants and increased the lignin content.

3.3. Metabolic changes in rice seedlings

The metabolites in the CK, 100NPs, 100NPs-20HA, IP, IP-100NPs, and IP-100NPs-20HA groups were analyzed to determine the metabolic changes in rice, and 700 and 704 metabolites were identified in the roots and shoots, respectively. The metabolites of the six groups were compared by principal component analysis (Figs. S10a–b), which revealed clear differences in the metabolites of the five treatment groups (100NPs, 100NPs-20HA, IP, IP-100NPs, and IP-100NPs-20HA) relative to the CK group. Variable importance projection (VIP) and P-values were used to assess differences between the two groups, where a VIP value > 1 and a p value < 0.05 represented a statistically significant differential metabolite. In the roots, the metabolites of the five groups were significantly downregulated compared with the CK group. Particularly in the NP groups, the downregulated metabolites accounted for more than 70% of total differential metabolites (DMs) of roots (Table S1); in contrast, there were no obvious upward or downward trends for the differential metabolites of shoots under treatments (Table S2). There were 89 and 19 common DMs in the roots and shoots, respectively,

among the five treatment groups (Figs. S10c–d). These results suggest that rice roots are more susceptible to NP stress due to direct root absorption.

The Kyoto Encyclopedia of Genes and Genomes (KEGG) topological map shows the metabolic pathways with an impact value > 0.1 and p-value <0.05 (Figs. S11–12). The results showed that 23 and 13 metabolic pathways were labeled in the roots and shoots, respectively, in the five groups (Figs. S11–12). There were significant differences in alanine, aspartate and glutamate metabolism in roots and shoots between the five groups and CK. Alanine, aspartate, and glutamate metabolism are considered short catabolic pathways closely associated with plant tolerance/detoxification mechanisms (Neto et al., 2021; Zhang et al., 2022). Antibiotics and salt stress disturb alanine, aspartate and glutamate metabolism (Khan et al., 2021; Liu et al., 2024). Our data showed that alanine, aspartate and glutamate metabolism play important roles in the response of rice to exogenous (NP, IP, NP-IP/HA, and NP-IP-HA mixtures) stress. In the roots and shoots, seven DMs were enriched in this pathway, most of which were involved in the tricarboxylic acid cycle and amino acid synthesis. In the roots, the expression of citrate and L-asparagine in the NP groups were lower than that of the CK; in the shoots, L-asparagine and L-glutamine were significantly downregulated (Table S3). The presence of IP and HA further reduced the expression of these metabolites. Most DMs in alanine, aspartate, and glutamate metabolism pathway were downregulated, suggesting that NP stress inhibited this metabolic pathway. However, IP and HA had positive effects on NP stress. Citrate acts as an intermediate of the tricarboxylic acid cycle and can provide energy for respiration and other metabolic pathways (Mahmud et al., 2018). As a nitrogen transport compound, asparagine can be catabolized by deamidation and transamination to release nitrogen for amino acid and protein synthesis (Gaufichon et al., 2010). Glutamine is a building block in protein synthesis and an N donor in the biosynthesis of amino acids, nucleic acids, amino sugars and vitamin B coenzymes (Lee et al., 2023a). The three metabolites play an extremely important role in rice as precursors in response to stress stimulation and energy supply. The downregulation of alanine, aspartate and glutamate metabolism provides a possible explanation for NPs reducing the root protein content (Fig. 2c).

Furthermore, the DMs in the roots were significantly enriched in phenylpropanoid biosynthesis under NP stress, whereas there was no significant change in the IP group (Fig. S11). In addition to the IP group, the expression of coniferyl aldehyde, p-coumaraldehyde and sinapyl alcohol in the other NP-containing groups were significantly lower than those in the CK (Table S3). The presence of IP and HA further reduced the expression of these metabolites. As an intermediate component of lignin, the expression of these metabolites affects root lignin synthesis. Based on the lignin results (Fig. 2e), we speculated that an increase in the lignin content of the roots might be caused by the rapid conversion of large amounts of coniferyl aldehyde, p-coumaraldehyde, and sinapyl alcohol downstream under NP stress and that HA and IP participation were positively affected this process. Lignin is produced as a secondary metabolite in enormous amounts by the phenylpropyl pathway, and is considered to be an important phytoalexins in defense responses (Chen et al., 2013). It plays an important role in plant growth, tissue and organ development, lodging resistance, and response to biotic and abiotic stresses (Volpi et al., 2019). Our data indicated that the application of NPs affected lignin synthesis in rice root. In general, changes in metabolites are caused by changes in gene expression at the transcript level. Therefore, we focused on analyzing gene expression changes.

3.4. Transcriptomic analysis of rice seedlings

To obtain a comprehensive picture of the genetic response of rice to NPs exposure, we conducted a transcriptomic analysis of the harvested rice roots and shoots. By combining the metabolic results with realistic environmental conditions, 100NPs, IP-100NPs-20HA, and CK groups were selected. There were significant differences between the metabolites of the three groups. The 100NPs group represented the effect of NPs on rice under ideal conditions, and IP-100NPs-20HA represented more realistic conditions; therefore, these two groups were selected to conduct further genetic analyses. Compared to the CK, 145 and 1078 DEGs were detected in the roots in the 100NPs and IP-100NPs-20HA groups, respectively, and 192 and 3604 DEGs in the shoots, respectively (Fig. S13a). The principal component analysis of the transcriptomic data revealed clear separations between IP-100NPs-20HA and CK in the roots and shoots, whereas there was no clear separation between 100NPs and CK (Fig. S13b). Of the DEGs in the IP-100NPs-20HA group, 55 (3.25%) root and 131 (3.05%) shoot transcripts were common with the 100NPs treatment, respectively (Fig. S13c–d). Thus, NP stress changes the gene profile of rice plants, and IP and HA may further exacerbate this difference. The DEGs were annotated using Gene Ontology (GO) enrichment analysis. The dominant GO terms in the roots and shoots of the 100NPs and IP-100NPs-20HA were similar. The common DEGs were involved in different cellular components, biological processes, and molecular functions, including in cell part, membrane part, membrane, organelle, cellular process, metabolic process, catalytic activity, and binding (Fig. S14). The higher the number of DEGs, the greater the influence of the GO terms. The above enriched genes were more enriched in the IP-100NPs-20HA group than in the 100NPs group.

In addition, to identify the biological processes involved in NPs stress, a KEGG pathway analysis was performed separately for the DEGs. The DEGs in the roots and shoots of the two groups were significantly enriched in phenylpropanoid biosynthesis compared to CK (Fig. S15). Moreover, glycolysis/gluconeogenesis and propanoate metabolism were significantly enriched in roots treated with 100NPs and IP-100NPs-20HA, while the MAPK signaling pathway-plant, glycerolipid metabolism, and linoleic acid metabolism pathways were significantly enriched in the shoots (Fig. S15). In summary, phenylpropanoid biosynthesis was found to be an overrepresented KEGG pathway. Similar to the metabolic result, these results showed that phenylpropanoid biosynthesis was altered during NPs treatment.

3.5. Conjoint omics analysis of NP-induced stress on rice

To further explore the relationship between DEGs and DMs in rice roots and shoots in response to NP exposure, a conjoint analysis of the transcriptome and metabolome was conducted to compare those of the 100NPs and IP-100NPs-20HA groups versus the CK. Significantly enriched DEGs and DM pathways were observed in the rice roots but not in the shoots in the two treatment groups. The DEGs and DMs in the roots of 100NPs were enriched in the pathways “Phenylpropanoid biosynthesis,” “Arginine biosynthesis,” and “Alanine, aspartate, and glutamate metabolism,” and they exhibited consistent expression patterns with significant differences (p-value <0.05) compared to the CK (Fig. S16a). In the IP-100NPs-20HA group, the DEGs and DMs were enriched in the pathways “Phenylpropanoid biosynthesis,” “Arginine biosynthesis,” “Alanine, aspartate, and glutamate metabolism,” “Tryptophan metabolism,” “Phenylalanine metabolism,” “Glyoxylate and dicarboxylate metabolism,” and “Phenylalanine, tyrosine, and tryptophan biosynthesis.” (Fig. S16b) Among these, the phenylpropanoid biosynthesis and amino acid metabolic pathways, including arginine biosynthesis and alanine, aspartate, glutamate metabolism, differed significantly between the treatment groups and CK (p-value <0.05), with phenylalanine biosynthesis exhibiting an extremely significant difference (p-value <0.01). Therefore, a network analysis of DEGs and DMs annotated in the arginine biosynthesis, alanine, aspartate, and glutamate metabolism, and phenylpropanoid biosynthesis pathways was conducted (Fig. 3, Fig. S17).

Arginine biosynthesis, and alanine, aspartate, and glutamate metabolism consisted of six DMs and 12 DEGs, most of which were connected to amino acid synthesis (Fig. S17, Table S4). The expression of five amino acids (including L-asparagine, L-argininosuccinate, L-aspartate,

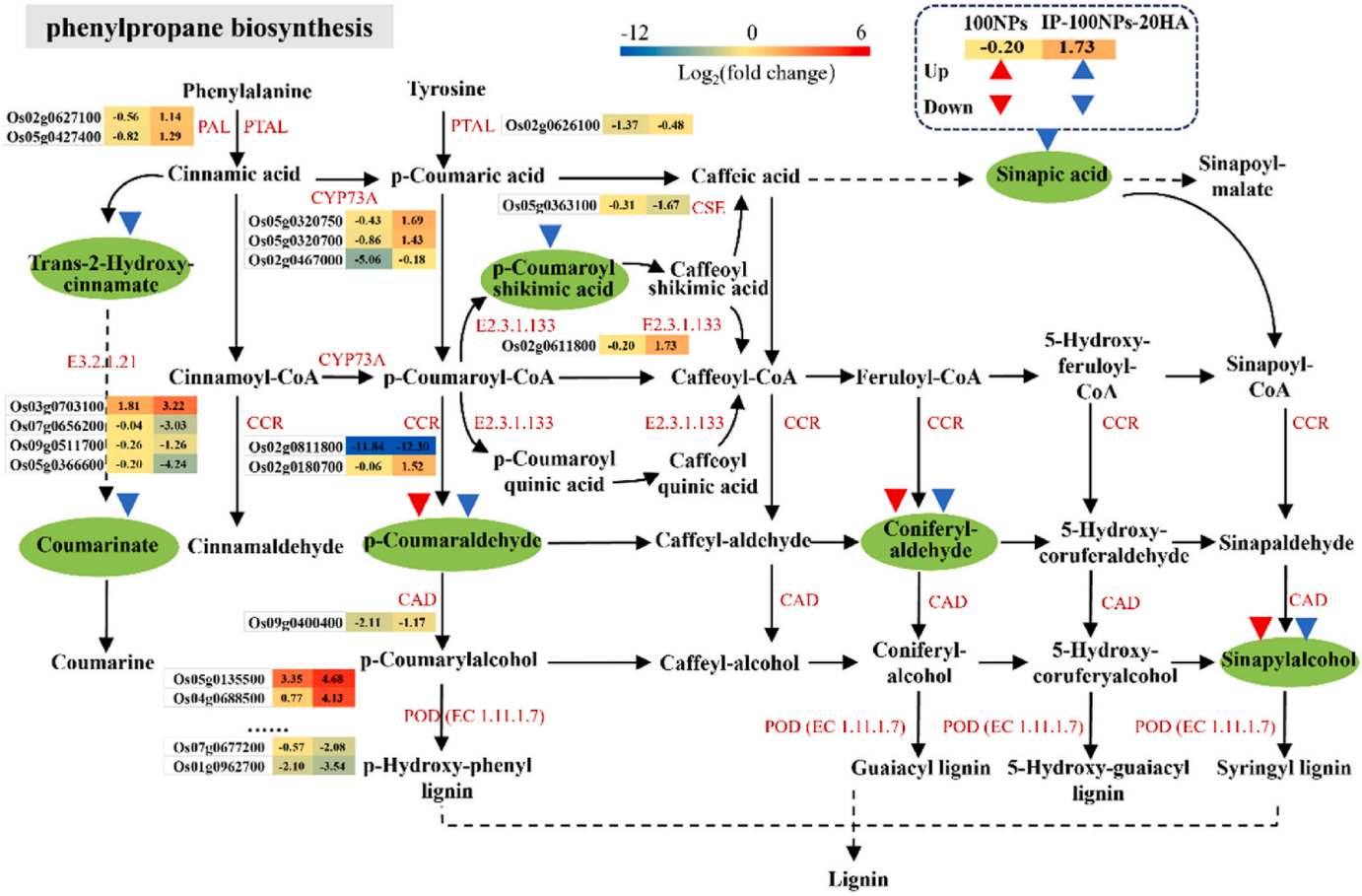

Fig. 3. DEGs and metabolites involved in phenylpropanoid biosynthesis pathway within rice (*Oryza sativa* L.) roots under 100NPs and IP-100NPs-20HA. Enzymes were marked in red and genes encoding the enzymes are annotated next to them. The relative contents of the gene expressions were presented in the form of a heat map (from low to high as presented in the color scale). The metabolite name in green indicates significantly regulated phenylpropanoid pathway intermediates, and the red and blue triangles show the regulation of metabolites in 100NPs and IP-100NPs-20HA, respectively. PAL (phenylalanine ammonia-lyase); PTAL (Similar to phenylalanine ammonia-lyase); CYP73A (trans-cinnamate 4-monooxygenase); CSE (Similar to monoglyceride lipase); HCT (shikimate O-hydroxycinnamoyl-transferase); CCR (cinnamoyl-CoA reductase); CAD (cinnamoyl alcohol dehydrogenase); POD (peroxidase). (For interpretation of the references to color in this figure legend, the reader is referred to the Web version of this article.)

citrate, and L-glutamine) in the two treatment groups was lower than those in the CK, but N-acetylornithine was comparatively increased in the CK (Fig. S17). L-asparagine and citrate were significantly down-regulated in all treatment groups (Fig. S17). For DEGs, only L-asparaginase (Os04g0650700) was upregulated, while the rest of the genes, aspartate aminotransferase (Os06g0548000, Os01g0760600), alanine transaminase (Os10g0390500, Os07g0108300), alanine-glyoxylate transaminase (Os05g0475400, Os08g0502700), aminoacylase (Os08g0511900), arginase (Os04g0106300), asparagine synthase (Os03g0291500), 4-aminobutyrate-pyruvate transaminase (Os04g0614600), and carbamoyl-phosphate synthase/aspartate carbamoyltransferase/dihydroorotase (Os01g0570700) were downregulated (Fig. S17). Regulation of the above coding genes was more obvious in the IP-100NPs-20HA group than in the 100NPs group. This suggests that NP stress may have negative effects on arginine biosynthesis, and alanine, aspartate, and glutamate metabolism, while IP and HA positively affected NP stress. A previous study also found that PS NPs can interfere with alanine, aspartate and glutamate metabolism in the corn (*Zea mays* L.) seedlings (Zhang et al., 2022). The arginine biosynthesis and alanine, aspartate, and glutamate metabolism are significantly decreased in the algae *Chlorella pyrenoidosa* (*C. pyrenoidosa*) under exposure to silver nanoparticles, hematite nanoparticles, and their mixtures (Cao et al., 2022). In the IP-100NPs-20HA group, DMs and DEGs were also accumulated in the other four pathways (including tryptophan metabolism, phenylalanine metabolism, phenylalanine, tyrosine and tryptophan biosynthesis, and glyoxylate and dicarboxylate metabolism) (Table S4). The four pathways consisted of 12 DMs and 39 DEGs, most of which were downregulated (Table S4). Tryptophan metabolism, phenylalanine metabolism, phenylalanine, tyrosine and tryptophan biosynthesis, and glyoxylate and dicarboxylate metabolism are the main amino acid and carbohydrate metabolism pathways, indicating that the presence of IP and HA negatively affected amino acid and carbohydrate metabolism under NP stress. The downregulation of these amino acid metabolic pathways also provided a possible explanation for the lower root protein content in the IP-100NPs-20HA group than in 100NPs group (Fig. 2c).

Several secondary metabolites, including lignin and other phenolic compounds, are derived from multiple branches of the phenylpropanoid pathway. In this study, phenylpropanoid biosynthesis consisted of six DMs and 38 DEGs, and all DMs were downregulated (Fig. 3, Table S4). Of these, p-coumaraldehyde, coniferyl aldehyde, and sinapyl alcohol were significantly downregulated and negatively regulated by the genes encoding cinnamoyl-CoA reductase (CCR) and cinnamylalcohol dehydrogenase (CAD) in the two treatment groups (Fig. 3). The genes encoding CCR (Os02g0811800) were downregulated by 3673.86- and 5056.70-fold in 100NPs and IP-100NPs-20HA, respectively, whereas CAD was downregulated by 4.32- and 2.45-fold, respectively (Fig. 3). Therein, CCR catalyzes the conversion of P-cinnamoyl CoA to p-coumaraldehyde and feruloyl-COA to coniferyl aldehyde, while CAD catalyzes the conversion of sinapaldehyde to sinapyl alcohol, which is an

important step in the lignin-specific branch of phenylpropanoid biosynthesis. However, most DEGs encoding Peroxidases (POD) were affected by NP and mixed NP/IP/HA stress, which are considered crucial for lignin formation. Among the 23 categories of POD identified, 13 genes were significantly upregulated and 10 genes were downregulated in 100NPs; however, 19 genes were significantly upregulated and 4 genes were downregulated in IP-100NPs-20HA. The overall expression of POD-related genes was upregulated in both groups, with Os05g0135500 and Os04g0688500 showing particularly significant increases. Os05g0135500 was upregulated by up to 10.19- and 25.68-fold, and Os04g0688500 was upregulated by up to 1.17- and 17.47-fold in 100NPs and IP-100NPs-20HA, respectively (Fig. 3, Table S5). An increase in the POD gene expression and the downregulation of upstream metabolites (sinapylalcohol) indicates that the phenylpropanoid biosynthesis pathway was activated by the NP and mixed NP/IP/HA treatments. These upregulated genes may lead to a rapid increase in the corresponding enzyme activity and the production of many secondary metabolites. The DEGs encoding POD were key genes regulating the synthesis of three monomers (p-hydroxy-phenyl lignin, guaiacyl lignin, 5-hydroxy-guaiacyl lignin, and syringyl lignin). However, there were no significant changes in POD activity (Fig. S7c), p-Hydroxy-phenyl lignin, guaiacyl lignin, 5-hhydroxy-guaiacyl lignin, or syringyl lignin (Fig. 3), suggesting that these newly generated metabolites were used as substrates to enter the lignin synthesis pathway via the action of POD. This was further confirmed by the increased lignin content (Fig. 2e). Consequently, NPs treatment promoted the accumulation of lignin in rice roots. Lignin is a polyphenolic polymer, and involved in the synthesis of secondary cytoderm (Alber et al., 2019). It confers plant structural integrity, assists in water transport, and contributes to plant defense mechanisms (Baxter et al., 2013). Similarly, NP treatment was found to activate the phenylpropanoid biosynthesis pathway, resulting in lignin and flavonoid accumulation in cotton roots (Li et al., 2024). NP stress enhances the process of deposition and polymerization of lignin and suberin monomers in the secondary wall, resulting in the formation of fortified secondary walls in exodermis, sclerenchyma, endodermis, and metaxylem cells (Yin et al., 2024). The thickened cell wall not only enhances the hardness of plants and promotes the formation of a physical barrier, but also reduces the permeability of cells to NPs (Song et al., 2021; Li et al., 2024). Furthermore, as lignin polymer contains a number of functional groups such as hydroxyl, carboxyl, methoxyl, and aldehyde groups (Guo et al., 2008), it may bind charged NPs, and reduce the entry of NPs into the cytoplasm. This could represent a defense mechanism in rice for coping with NP stress. A previous study found that the lignification of cell walls to form a physical barrier can reduce cadmium uptake by cotton (Chen et al., 2019).

In addition to the downregulation of p-coumaraldehyde, coniferyl aldehyde, and sinapyl alcohol and the upregulation of POD-related genes, trans-2-hydroxy-cinnamate, coumarinate, P-coumaroyl shikimic acid, and sinapic acid were significantly downregulated in the IP-100NPs-20HA group. The corresponding DEGs encoding shikimate O-hydroxycinnamoyltransferase (HCT), phenylalanine ammonia-lyase (PAL), and trans-cinnamate 4-monooxygenase (CYP73A) were also significantly upregulated (Fig. 3, Table S5). This finding indicated that HA and IP positively affected the phenylpropanoid biosynthesis under NP stress and further activated this pathway and promoted lignin synthesis, which may be a possible reason for the higher root lignin content in the IP-100NPs-20HA group compared with the 100NPs group (Fig. 2e). Overall, the phenylpropanoid biosynthesis plays a key role in resisting NP stress in rice, and IP and HA had positive effects on NPs-induced phenylpropanoid biosynthesis.

4. Conclusions

In this study, we demonstrated the uptake of NPs by rice root in the presence of IP and HA and their effects on rice by analyzing the morphological and biochemical indices and omics. NPs decreased SOD activity (28.9–44.0%) and the protein content levels (32.2–38.6%) and altered the gene expression and metabolite profile of the roots. IP and HA further decreased root protein contents and increased root lignin contents. IP alleviated NP-induced oxidative stress on the roots, whereas HA had the opposite effect. The transcriptomic and metabolomic results revealed that NPs significantly inhibited arginine biosynthesis and alanine, aspartate, and glutamate metabolism and activated phenylpropanoid biosynthesis. The coexistence of IP and HA positively affected the amino acid and carbohydrate metabolism and phenylpropanoid biosynthesis induced by NPs in rice roots. The inhibition of amino acid metabolism may affect protein biosynthesis and thus lead to a decrease in the root protein content. The activation of phenylpropanoid biosynthesis caused an increase in the root lignin content as a secondary metabolite, which promoted the formation of apoplastic barriers, ultimately inhibiting the absorption and transport of NPs. In summary, NPs pose a large risk to rice plants; however, naturally occurring minerals and HA in the rhizosphere environment may influence their environmental risk. Therefore, when predicting the fate and toxicity of NPs at the solution-plant interface, the effects of coexisting minerals and HA as well as environmental conditions should be considered. Additional parameters should also be considered to elucidate the fate of NPs under real environmental conditions. Nevertheless, our providing important data and aid in the prediction of the geochemical behavior and biotoxicity of NPs in aquatic environments in the presence of minerals and HA.

CRediT authorship contribution statement

Xiaoxue Ouyang: Writing – review & editing, Writing – original draft, Investigation. **Jie Ma:** Writing – review & editing, Writing – original draft, Methodology, Investigation. **Bingcong Feng:** Investigation. **Yong Liu:** Investigation. **Ping Yin:** Investigation. **Xiaoyu Zhang:** Investigation. **Pan Li:** Writing – review & editing. **Qiusheng Chen:** Supervision. **Yujie Zhao:** Supervision. **Liping Weng:** Supervision, Project administration. **Yongtao Li:** Supervision.

Declaration of competing interest

The authors declare that they have no known competing financial interests or personal relationships that could have appeared to influence the work reported in this paper.

Acknowledgments

The study is financially supported by the National Natural Science Foundation of China (No. 42377409 and 42307511), Natural Science Foundation of Tianjin (23JCYBJC00310) and Science and Technology Innovation Project of Chinese Academy of Agricultural Sciences.

Appendix A. Supplementary data

Supplementary data to this article can be found online at https://doi.org/10.1016/j.envpol.2024.125246.

Data availability

No data was used for the research described in the article.

References

Adeleye, A.T., Bahar, M.M., Megharaj, M., Rahman, M.M., 2023. Recent developments and mechanistic insights on adsorption technology for micro- and nanoplastics removal in aquatic environments. J. Water Proc. Eng. 53. https://doi.org/10.1016/j.jwpe.2023.103777.

Alber, A.V., Renault, H., Basilio-Lopes, A., Bassard, J.E., Liu, Z., Ullmann, P., Lesot, A., Bihel, F., Schmitt, M., Werck-Reichhart, D., Ehlting, J., 2019. Evolution of coumaroyl

conjugate 3-hydroxylases in land plants: lignin biosynthesis and defense. Plant J. 99, 924–936. https://doi.org/10.1111/tpj.14373.
Atugoda, T., Piyumali, H., Wijesekara, H., Sonne, C., Lam, S.S., Mahatantila, K., Vithanage, M., 2022. Nanoplastic occurrence, transformation and toxicity: a review. Environ. Chem. Lett. 21, 363–381. https://doi.org/10.1007/s10311-022-01479-w.
Baxter, H.L., Neal, C., Jr, S.J.B., 2013. Effects of Altered Lignin Biosynthesis on Phenylpropanoid Metabolism and Plant Stress, vol. 4, pp. 635–650.
Black, B.D., Harrington, G.W., Singer, P.C., 1996. Reducing cancer risks by improving organic carbon removal. J. AWWA (Am. Water Works Assoc.) 88, 40–52. https://doi.org/10.1002/j.1551-8833.1996.tb06570.x.
Cao, M., Wang, F., Zhou, B., Chen, H., Yuan, R., Ma, S., Geng, H., Xing, B., 2022. Mechanisms of photoinduced toxicity of AgNPs to the microalgae Chlorella pyrenoidosa in the presence of hematite nanoparticles: insights from transcriptomics, metabolomics and the photochemical index. Environ. Sci.: Nano 9, 3525–3537. https://doi.org/10.1039/d2en00450j.
Chae, Y., An, Y.-J., 2020. Nanoplastic ingestion induces behavioral disorders in terrestrial snails: trophic transfer effect via vascular plants. Environ. Sci.: Nano 7. https://doi.org/10.1039/C9EN01335K.
Chen, H., Li, Y., Ma, X., Guo, L., He, Y., Ren, Z., Kuang, Z., Zhang, X., Zhang, Z., 2019. Analysis of potential strategies for cadmium stress tolerance revealed by transcriptome analysis of upland cotton. Sci. Rep. 9, 86. https://doi.org/10.1038/s41598-018-36228-z.
Chen, W., Gong, L., Guo, Z., Wang, W., Zhang, H., Liu, X., Yu, S., Xiong, L., Luo, J., 2013. A novel integrated method for large-scale detection, identification, and quantification of widely targeted metabolites: application in the study of rice metabolomics. Mol. Plant 6, 1769–1780. https://doi.org/10.1093/mp/sst080.
Day, A., Neutelings, G., Nolin, F., Grec, S., Habrant, A., Crônier, D., Maher, B., Rolando, C., David, H., Chabbert, B., Hawkins, S., 2009. Caffeoyl coenzyme A O-methyltransferase down-regulation is associated with modifications in lignin and cell-wall architecture in flax secondary xylem. Plant Physiol. Biochem. 47, 9–19. https://doi.org/10.1016/j.plaphy.2008.09.011.
Dong, S., Cai, W., Xia, J., Sheng, L., Wang, W., Liu, H., 2021. Aggregation kinetics of fragmental PET nanoplastics in aqueous environment: complex roles of electrolytes, pH and humic acid. Environ. Pollut. 268, 115828. https://doi.org/10.1016/j.envpol.2020.115828.
Dong, Y., Gao, M., Song, Z., Qiu, W., 2020. Microplastic particles increase arsenic toxicity to rice seedlings. Environ. Pollut. 259, 113892. https://doi.org/10.1016/j.envpol.2019.113892.
Fu, Y., Yang, X., Shen, H., 2018. Root iron plaque alleviates cadmium toxicity to rice (Oryza sativa) seedlings. Ecotoxicol. Environ. Saf. 161, 534–541. https://doi.org/10.1016/j.ecoenv.2018.06.015.
Gao, M., Wang, Z., Jia, Z., Zhang, H., Wang, T., 2023. Brassinosteroids alleviate nanoplastic toxicity in edible plants by activating antioxidant defense systems and suppressing nanoplastic uptake. Environ. Int. 174, 107901. https://doi.org/10.1016/j.envint.2023.107901.
Gaufichon, L., Reisdorf-Cren, M., Rothstein, S.J., Chardon, F., Suzuki, A., 2010. Biological functions of asparagine synthetase in plants. Plant Sci. 179, 141–153. https://doi.org/10.1016/j.plantsci.2010.04.010.
Gigault, J., Halle, A.T., Baudrimont, M., Pascal, P.Y., Gauffre, F., Phi, T.L., El Hadri, H., Grassl, B., Reynaud, S., 2018. Current opinion: what is a nanoplastic? Environ. Pollut. 235, 1030–1034. https://doi.org/10.1016/j.envpol.2018.01.024.
Giorgetti, L., Spano, C., Muccifora, S., Bottega, S., Barbieri, F., Bellani, L., Ruffini Castiglione, M., 2020. Exploring the interaction between polystyrene nanoplastics and Allium cepa during germination: internalization in root cells, induction of toxicity and oxidative stress. Plant Physiol. Biochem. 149, 170–177. https://doi.org/10.1016/j.plaphy.2020.02.014.
Guo, X., Zhang, S., Shan, X.Q., 2008. Adsorption of metal ions on lignin. J. Hazard Mater. 151, 134–142. https://doi.org/10.1016/j.jhazmat.2007.05.065.
Hartmann, G.F., Ricachenevsky, F.K., Silveira, N.M., Pita-Barbosa, A., 2022. Phytotoxic effects of plastic pollution in crops: what is the size of the problem? Environ. Pollut. 292, 118420. https://doi.org/10.1016/j.envpol.2021.118420.
Hemati, A., Alikhani, H., Bagheri Marandi, G., 2012. Extractants and Extraction Time Effects on Physicochemical Properties of Humic Acid, vol. 2, pp. 975–984.
Jia, Y., Xu, L., Wang, X., Demopoulos, G.P., 2007. Infrared spectroscopic and X-ray diffraction characterization of the nature of adsorbed arsenate on ferrihydrite. Geochim Cosmochim Acta 71, 1643–1654. https://doi.org/10.1016/j.gca.2006.12.021.
Jiang, M., Wang, B., Ye, R., Yu, N., Xie, Z., Hua, Y., Zhou, R., Tian, B., Dai, S., 2022. Evidence and impacts of nanoplastic accumulation on crop grains. Adv. Sci. 9. https://doi.org/10.1002/advs.202202336.
Jiang, X., Chen, H., Liao, Y., Ye, Z., Li, M., Klobucar, G., 2019. Ecotoxicity and genotoxicity of polystyrene microplastics on higher plant Vicia faba. Environ. Pollut. 250, 831–838. https://doi.org/10.1016/j.envpol.2019.04.055.
Junaid, M., Wang, J., 2021. Interaction of nanoplastics with extracellular polymeric substances (EPS) in the aquatic environment: a special reference to eco-corona formation and associated impacts. Water Res. 201, 117319. https://doi.org/10.1016/j.watres.2021.117319.
Kang, S., Xing, B., 2008. Humic acid fractionation upon sequential adsorption onto goethite. Langmuir 24, 2525–2531. https://doi.org/10.1021/la702914q.
Kärkönen, A., Koutaniemi, S., 2010. Lignin biosynthesis studies in plant tissue cultures. J. Integr. Plant Biol. 52, 176–185. https://doi.org/10.1111/j.1744-7909.2010.00913.x.
Khan, k.Y., Ali, B., Zhang, S., Stoffella, P., Yuan, S., Xia, Q., Qu, H., Shi, Y., Cui, X., Guo, Y., 2021. Effects of antibiotics stress on growth variables, ultrastructure, and metabolite pattern of Brassica rapa ssp. Chinensis. Sci. Total Environ. 778, 146333. https://doi.org/10.1016/j.scitotenv.2021.146333.
Lee, K.T., Liao, H.S., Hsieh, M.H., 2023a. Glutamine metabolism, sensing and signaling in plants. Plant Cell Physiol. 64, 1466–1481. https://doi.org/10.1093/pcp/pcad054.
Lee, Y., Cho, S., Park, K., Kim, T., Kim, J., Ryu, D.Y., Hong, J., 2023b. Potential lifetime effects caused by cellular uptake of nanoplastics: a review. Environ. Pollut. 329, 121668. https://doi.org/10.1016/j.envpol.2023.121668.
Lei, C., Engeseth, N.J., 2022. Comparison of growth and quality between hydroponically grown and soil-grown lettuce under the stress of microplastics. ACS ES&T Water 2, 1182–1194. https://doi.org/10.1021/acsestwater.1c00485.
Li, F., Guo, H., Zhou, X., Zhao, K., Shen, J., Liu, F., Wei, C., 2017a. Impact of natural organic matter on arsenic removal by modified granular natural siderite: evidence of ternary complex formation by HPSEC-UV-ICP-MS. Chemosphere 168, 777–785. https://doi.org/10.1016/j.chemosphere.2016.10.135.
Li, L., Luo, Y., Li, R., Zhou, Q., Peijnenburg, W.J.G.M., Yin, N., Yang, J., Tu, C., Zhang, Y., 2020. Effective uptake of submicrometre plastics by crop plants via a crack-entry mode. Nat. Sustain. 3, 929–937. https://doi.org/10.1038/s41893-020-0567-9.
Li, M., He, L., Zhang, M., Liu, X., Tong, M., Kim, H., 2019. Cotransport and deposition of iron oxides with different-sized plastic particles in saturated quartz sand. Environ. Sci. Technol. 53, 3547–3557. https://doi.org/10.1021/acs.est.8b06904.
Li, R.R., Wang, B.L., Nan, F.R., Lv, J.P., Liu, X.D., Liu, Q., Feng, J., Xie, S.L., 2023. Effects of polystyrene nanoplastics on the physiological and biochemical characteristics of microalga Scenedesmusquadricauda. Environ. Pollut. 319, 120987. https://doi.org/10.1016/j.envpol.2022.120987.
Li, S., Liu, H., Gao, R., Abdurahman, A., Dai, J., Zeng, F., 2018. Aggregation kinetics of microplastics in aquatic environment: complex roles of electrolytes, pH, and natural organic matter. Environ. Pollut. 237, 126–132. https://doi.org/10.1016/j.envpol.2018.02.042.
Li, W., Zhao, J., Zhang, Z., Ren, Z., Li, X., Zhang, R., Ma, X., 2024. Uptake and effect of carboxyl-modified polystyrene microplastics on cotton plants. J. Hazard Mater. 466. https://doi.org/10.1016/j.jhazmat.2024.133581.
Li, W.C., Deng, H., Wong, M.H., 2017b. Effects of Fe plaque and organic acids on metal uptake by wetland plants under drained and waterlogged conditions. Environ. Pollut. 231, 732–741. https://doi.org/10.1016/j.envpol.2017.08.012.
Li, Y., Zhao, J., Zhang, B., Liu, Y., Xu, X., Li, Y.-F., Li, B., Gao, Y., Chai, Z., 2016. The influence of iron plaque on the absorption, translocation and transformation of mercury in rice (Oryza sativa L.) seedlings exposed to different mercury species. Plant Soil 398, 87–97. https://doi.org/10.1007/s11104-015-2627-x.
Li, Z., Li, Q., Li, R., Zhou, J., Wang, G., 2021. The distribution and impact of polystyrene nanoplastics on cucumber plants. Environ. Sci. Pollut. Control Ser. 28, 16042–16053. https://doi.org/10.1007/s11356-020-11702-2.
Lian, J., Liu, W., Meng, L., Wu, J., Chao, L., Zeb, A., Sun, Y., 2021. Foliar-applied polystyrene nanoplastics (PSNPs) reduce the growth and nutritional quality of lettuce (Lactuca sativa L.). Environ. Pollut. 280, 116978. https://doi.org/10.1016/j.envpol.2021.116978.
Lian, J., Wu, J., Xiong, H., Zeb, A., Yang, T., Su, X., Su, L., Liu, W., 2020. Impact of polystyrene nanoplastics (PSNPs) on seed germination and seedling growth of wheat (Triticum aestivum L.). J. Hazard Mater. 385, 121620. https://doi.org/10.1016/j.jhazmat.2019.121620.
Liao, H.-S., Chung, Y.-H., Hsieh, M.-H., 2022. Glutamate: a multifunctional amino acid in plants. Plant Sci. 318. https://doi.org/10.1016/j.plantsci.2022.111238.
Lima, J.Z., Cassaro, R., Ogura, A.P., Vianna, M.M.G.R., 2023. A systematic review of the effects of microplastics and nanoplastics on the soil-plant system. Sustain. Prod. Consum. 38, 266–282. https://doi.org/10.1016/j.spc.2023.04.010.
Liu, N., Lou, X., Li, X., Shuai, Z., Liu, H., Jiang, Z., Wei, S., 2021a. Rhizosphere dissolved organic matter and iron plaque modified by organic amendments and its relations to cadmium bioavailability and accumulation in rice. Sci. Total Environ. 792, 148216. https://doi.org/10.1016/j.scitotenv.2021.148216.
Liu, S., Wang, J., Zhu, J., Wang, J., Wang, H., Zhan, X., 2021b. The joint toxicity of polyethylene microplastic and phenanthrene to wheat seedlings. Chemosphere 282. https://doi.org/10.1016/j.chemosphere.2021.130967.
Liu, Y., Guo, R., Zhang, S., Sun, Y., Wang, F., 2022. Uptake and translocation of nano/microplastics by rice seedlings: evidence from a hydroponic experiment. J. Hazard Mater. 421, 126700. https://doi.org/10.1016/j.jhazmat.2021.126700.
Liu, Y., Zheng, J., Ge, L., Tang, H., Hu, J., Li, X., Wang, X., Zhang, Y., Shi, Q., 2024. Integrated metabolomic and transcriptomic analyses reveal the roles of alanine, aspartate and glutamate metabolism and glutathione metabolism in response to salt stress in tomato. Sci. Hortic. 328. https://doi.org/10.1016/j.scienta.2024.112911.
Ma, J., Guo, H., Lei, M., Li, Y., Weng, L., Chen, Y., Ma, Y., Deng, Y., Feng, X., Xiu, W., 2018a. Enhanced transport of ferrihydrite colloid by chain-shaped humic acid colloid in saturated porous media. Sci. Total Environ. 621, 1581–1590. https://doi.org/10.1016/j.scitotenv.2017.10.070.
Ma, J., Guo, H., Weng, L., Li, Y., Lei, M., Chen, Y., 2018b. Distinct effect of humic acid on ferrihydrite colloid-facilitated transport of arsenic in saturated media at different pH. Chemosphere 212, 794–801. https://doi.org/10.1016/j.chemosphere.2018.08.131.
Ma, J., Qiu, Y., Zhao, J., Ouyang, X., Zhao, Y., Weng, L., Md Yasir, A., Chen, Y., Li, Y., 2022. Effect of agricultural organic inputs on nanoplastics transport in saturated goethite-coated porous media: particle size selectivity and role of dissolved organic matter. Environ. Sci. Technol. 56, 3524–3534. https://doi.org/10.1021/acs.est.1c07574.
Mahmud, J.A., Hasanuzzaman, M., Nahar, K., Bhuyan, M., Fujita, M., 2018. Insights into citric acid-induced cadmium tolerance and phytoremediation in Brassica juncea L.: coordinated functions of metal chelation, antioxidant defense and glyoxalase systems. Ecotoxicol. Environ. Saf. 147, 990–1001. https://doi.org/10.1016/j.ecoenv.2017.09.045.
Maity, S., Chatterjee, A., Guchhait, R., De, S., Pramanick, K., 2020. Cytogenotoxic potential of a hazardous material, polystyrene microparticles on Allium cepa L. J. Hazard Mater. 385, 121560. https://doi.org/10.1016/j.jhazmat.2019.121560.

Mao, Y., Ai, H., Chen, Y., Zhang, Z., Zeng, P., Kang, L., Li, W., Gu, W., He, Q., Li, H., 2018. Phytoplankton response to polystyrene microplastics: perspective from an entire growth period. Chemosphere 208, 59–68. https://doi.org/10.1016/j.chemosphere.2018.05.170.

Neto, J.C.R., Vieira, L.R., de Aquino Ribeiro, J.A., de Sousa, C.A.F., Junior, M.T.S., Abdelnur, P.V., 2021. Metabolic effect of drought stress on the leaves of young oil palm (Elaeis guineensis) plants using UHPLC-MS and multivariate analysis. Sci. Rep. 11, 18271. https://doi.org/10.1038/s41598-021-97835-x.

Nie, X., Xing, X., Xie, R., Wang, J., Yang, S., Wan, Q., Zeng, E.Y., 2023. Impact of iron/aluminum (hydr)oxide and clay minerals on heteroaggregation and transport of nanoplastics in aquatic environment. J. Hazard Mater. 446. https://doi.org/10.1016/j.jhazmat.2022.130649.

Prust, M., Meijer, J., Westerink, R.H.S., 2020. The plastic brain: neurotoxicity of micro- and nanoplastics. Part. Fibre Toxicol. 17, 24. https://doi.org/10.1186/s12989-020-00358-y.

Qian, X., Ma, J., Weng, L., Chen, Y., Ren, Z., Li, Y., 2020. Influence of agricultural organic inputs and their aging on the transport of ferrihydrite nanoparticles: from enhancement to inhibition. Sci. Total Environ. 719, 137440. https://doi.org/10.1016/j.scitotenv.2020.137440.

Quevedo, I.R., Olsson, A.L., Tufenkji, N., 2013. Deposition kinetics of quantum dots and polystyrene latex nanoparticles onto alumina: role of water chemistry and particle coating. Environ. Sci. Technol. 47, 2212–2220. https://doi.org/10.1021/es303392v.

Sebastian, A., Prasad, M.N.V., 2016. Iron plaque decreases cadmium accumulation in Oryza sativa L. and serves as a source of iron. Plant Biol 18, 1008–1015. https://doi.org/10.1111/plb.12484.

Shen, M., Zhang, Y., Zhu, Y., Song, B., Zeng, G., Hu, D., Wen, X., Ren, X., 2019. Recent advances in toxicological research of nanoplastics in the environment: a review. Environ. Pollut. 252, 511–521. https://doi.org/10.1016/j.envpol.2019.05.102.

Song, Z., Wang, D., Gao, Y., Li, C., Jiang, H., Zhu, X., Zhang, H., 2021. Changes of lignin biosynthesis in tobacco leaves during maturation. Funct. Plant Biol. 48. https://doi.org/10.1071/fp20244.

Sun, H., Lei, C., Xu, J., Li, R., 2021. Foliar uptake and leaf-to-root translocation of nanoplastics with different coating charge in maize plants. J. Hazard Mater. 416, 125854. https://doi.org/10.1016/j.jhazmat.2021.125854.

Sun, X., Yuan, X.-Z., Jia, Y., Feng, L., Zhu, F.-P., Dong, S.-S., Liu, J., Kong, X., Tian, H., Duan, J.-L., Ding, Z., Wang, S.-G., Xing, B., 2020. Differentially charged nanoplastics demonstrate distinct accumulation in Arabidopsis thaliana. Nat. Nanotechnol. 15. https://doi.org/10.1038/s41565-020-0707-4.

Tan, M., Liu, L., Zhang, M., Liu, Y., Li, C., 2021. Effects of solution chemistry and humic acid on the transport of polystyrene microplastics in manganese oxides coated sand. J. Hazard Mater. 413, 125410. https://doi.org/10.1016/j.jhazmat.2021.125410.

Valdrighi, M.M., Pera, A., Agnolucci, M., Frassinetti, S., Lunardi, D., Vallini, G., 1996. Effects of compost-derived humic acids on vegetable biomass production and microbial growth within a plant (Cichorium intybus)-soil system: a comparative study. Agric. Ecosyst. Environ. 58, 133–144. https://doi.org/10.1016/0167-8809(96)01031-6.

Volpi, E.S.N., Mazzafera, P., Cesarino, I., 2019. Should I stay or should I go: are chlorogenic acids mobilized towards lignin biosynthesis? Phytochemistry 166, 112063. https://doi.org/10.1016/j.phytochem.2019.112063.

Wang, D., Bradford, S.A., Harvey, R.W., Gao, B., Cang, L., Zhou, D., 2012. Humic acid facilitates the transport of ARS-labeled hydroxyapatite nanoparticles in iron oxyhydroxide-coated sand. Environ. Sci. Technol. 46, 2738–2745. https://doi.org/10.1021/es203784u.

Wang, F., Feng, X., Liu, Y., Adams, C.A., Sun, Y., Zhang, S., 2022a. Micro(nano)plastics and terrestrial plants: up-to-date knowledge on uptake, translocation, and phytotoxicity. Resour. Conserv. Recycl. 185. https://doi.org/10.1016/j.resconrec.2022.106503.

Wang, W., Yuan, W., Xu, E.G., Li, L., Zhang, H., Yang, Y., 2022b. Uptake, translocation, and biological impacts of micro(nano)plastics in terrestrial plants: progress and prospects. Environ. Res. 203, 111867. https://doi.org/10.1016/j.envres.2021.111867.

Ward, J.T., Lahner, B., Yakubova, E., Salt, D.E., Raghothama, K.G., 2008. The effect of iron on the primary root elongation of Arabidopsis during phosphate deficiency. Plant Physiol 147, 1181–1191. https://doi.org/10.1104/pp.108.118562.

Williams, P.N., Santner, J., Larsen, M., Lehto, N.J., Oburger, E., Wenzel, W., Glud, R.N., Davison, W., Zhang, H., 2014. Localized flux maxima of arsenic, lead, and iron around root apices in flooded lowland rice. Environ. Sci. Technol. 48, 8498–8506. https://doi.org/10.1021/es501127k.

Wu, H., Li, Z., 2022. Nano-enabled agriculture: how do nanoparticles cross barriers in plants? Plant Communications 3. https://doi.org/10.1016/j.xplc.2022.100346.

Xiong, J., Weng, L., Koopal, L.K., Wang, M., Shi, Z., Zheng, L., Tan, W., 2018. Effect of soil fulvic and humic acids on Pb binding to the goethite/solution interface: ligand charge distribution modeling and speciation distribution of Pb. Environ. Sci. Technol. 52, 1348–1356. https://doi.org/10.1021/acs.est.7b05412.

Yang, Y., Hu, H., Fu, Q., Zhu, J., Zhang, X., Xi, R., 2020. Phosphorus regulates as uptake by rice via releasing as into soil porewater and sequestrating it on Fe plaque. Sci. Total Environ. 738, 139869. https://doi.org/10.1016/j.scitotenv.2020.139869.

Yin, J., Zhu, T., Li, X., Yin, X., Xu, J., Xu, G., 2024. Polystyrene nanoplastics induce cell type-dependent secondary wall reinforcement in rice (Oryza sativa) roots and reduce root hydraulic conductivity. J. Hazard Mater. 477. https://doi.org/10.1016/j.jhazmat.2024.135309.

Zhang, T.-R., Wang, C.-X., Dong, F.-Q., Gao, Z.-Y., Zhang, C.-J., Zhang, X.-J., Fu, L.-M., Wang, Y., Zhang, J.-P., 2019. Uptake and translocation of styrene maleic anhydride nanoparticles in murraya exotica plants as revealed by noninvasive, real-time optical bioimaging. Environ. Sci. Technol. 53, 1471–1481. https://doi.org/10.1021/acs.est.8b05689.

Zhang, Y., Luo, Y., Guo, X., Xia, T., Wang, T., Jia, H., Zhu, L., 2020. Charge mediated interaction of polystyrene nanoplastic (PSNP) with minerals in aqueous phase. Water Res. 178, 115861. https://doi.org/10.1016/j.watres.2020.115861.

Zhang, Y., Yang, X., Luo, Z.-x., Lai, J.-l., Li, C., Luo, X.-g., 2022. Effects of polystyrene nanoplastics (PSNPs) on the physiology and molecular metabolism of corn (Zea mays L.) seedlings. Sci. Total Environ. 806. https://doi.org/10.1016/j.scitotenv.2021.150895.

Zhou, C.-Q., Lu, C.-H., Mai, L., Bao, L.-J., Liu, L.-Y., Zeng, E.Y., 2021. Response of rice (Oryza sativa L.) roots to nanoplastic treatment at seedling stage. J. Hazard Mater. 401, 123412. https://doi.org/10.1016/j.jhazmat.2020.123412.

Zuverza-Mena, N., Martinez-Fernandez, D., Du, W., Hernandez-Viezcas, J.A., Bonilla-Bird, N., Lopez-Moreno, M.L., Komarek, M., Peralta-Videa, J.R., Gardea-Torresdey, J.L., 2017. Exposure of engineered nanomaterials to plants: insights into the physiological and biochemical responses-A review. Plant Physiol. Biochem. 110, 236–264. https://doi.org/10.1016/j.plaphy.2016.05.037.